APL Photonics ARTICLE pubs.aip.org/aip/app

Gigawatt level, 10 fs high efficiency visible pulse generation

Cite as: APL Photon. 10, 080804 (2025); doi: 10.1063/5.0278034
Submitted: 27 April 2025 • Accepted: 11 August 2025 •
Published Online: 27 August 2025

Pedram Abdolghader,[1,a)] Marco Scaglia,[1] Étienne Doiron,[1] Maksym Ivanov,[1] Madhu Beniwal,[1,2] Gabriel Tempea,[1] Ximeng Zheng,[1,2] Pooya Abdolghader,[1,3] Giulio Vampa,[4,5] and Bruno E. Schmidt[1,b)]

AFFILIATIONS

[1] few-cycle Inc., 1650 Boulevard Lionel-Boulet, Varennes, Quebec J3X 1P7, Canada
[2] Institut National de la Recherche Scientifique, 1650 Boulevard Lionel-Boulet, Varennes, Quebec J3X 1P7, Canada
[3] Concordia University Department of Computer Science and Software Engineering, Montreal, Quebec H3H 2L9, Canada
[4] NRC-uOttawa Joint Centre for Extreme Photonics, Ottawa, Ontario K1N 6N5, Canada
[5] National Research Council of Canada, 100 Sussex drive, Ottawa, Ontario K1N 0R6, Canada

Note: This paper is part of the Special Topic on Advances Enabled by Ytterbium: From Advanced Laser Technology to Breakthrough Applications.
[a)] **Author to whom correspondence should be addressed:** abdolghaderpedram@gmail.com
[b)] **Electronic mail:** schmidt@few-cycle.com

ABSTRACT

We present a robust approach capable of generating ultrashort pulses in the visible (VIS) spectral range through second-harmonic generation of broadened pulses centered at around 1030 nm. Tunable VIS pulses with durations as short as 10 fs, sub-20 fs, and sub-50 fs across the 420–600 nm range are achieved by spectrally broadening the 1030 nm output employing a dual-stage hollow-core fiber setup, followed by frequency doubling in cascaded beta barium borate ($\beta - BaB_2O_4$, BBO) crystals. The system delivers pulse energies ranging from a few to above hundred microjoules at repetition rates ranging between 10 and 100 kHz, while maintaining excellent beam quality and power stability over several hours of continuous operation. These characteristics make the source highly suitable for applications in ultrafast spectroscopy, nonlinear optics, and strong-field physics.

I. INTRODUCTION

The availability of ultrashort, high-intensity laser pulses operating at high repetition rates has opened new frontiers in ultrafast science and advanced laser technologies. Ytterbium-doped laser technology has gained significant attention due to its unprecedented levels of average power (kilowatt level), repetition rates, and excellent stability over the past decade.[1–4] Although Yb-based laser systems typically exhibit longer pulse durations compared to Ti: sapphire lasers due to their limited gain bandwidth,[5,6] this drawback can be effectively mitigated. Pulse post-compression techniques, such as nonlinear spectral broadening via self-phase modulation (SPM), followed by phase compensation enable the generation of few-cycle pulses from Yb systems. The phase compensation is commonly achieved using chirped mirrors (CM). The first demonstration of pulse compression through spectral broadening in a hollow-core fiber (HCF) was reported in 1996.[7,8] Since then, various pulse post-compression schemes have been successfully implemented, including guided mode propagation in HCFs, repetitive refocusing according to a multi-pass cell (MPC) scheme, multiple thin plates, and cascaded focusing and compression.[9–21] Among various compression techniques, HCFs exhibit excellent scalability with both peak and average power. Notable advancements in power scaling include demonstrations of 70 mJ energy input at 1030 nm[22] and average powers reaching 580 W with 5.8 mJ pulses.[23] Recently, the efficiency of 1.4 mJ sub-two cycle compression employing a two stage HCF setup has reached 70%.[14]

In addition to facilitating pulse compression, HCF systems offer compelling features for ultrafast nonlinear optics. The extended interaction length, along with the flexibility to tailor the nonlinear medium through gas type, pressure, and gradient pressure techniques creates a versatile and controllable platform for advanced nonlinear experiments. To name a few notable advancements, these include sub-3 fs deep ultraviolet (UV) pulse generation via resonant dispersive wave (RDW) emission,[24] extreme self-compression based on soliton dynamics,[25] intense few-cycle visible pulse generation through nonlinear fiber mode mixing,[26] optimized spectral phase transfer in four-wave mixing,[27] and high-energy ultraviolet pulse generation via four-wave mixing, achieving conversion efficiencies approaching 50%.[28,29]

Generation of intense ultrashort pulses within the visible spectral range is relatively challenging and requires experimental efforts due to the intrinsic difficulty in managing chromatic dispersion and strong nonlinearities over broad bandwidths. Additional limitations arise from the efficiency of frequency conversion. In an influential study from the late 1980s, visible pulses at the nanojoule level, with central wavelengths between 500 and 650 nm, were generated with durations as short as 6 fs. This was achieved using a femtosecond dye laser, followed by further amplification and pulse compression stages.[30] To date, few-cycle (sub-10 fs) visible pulse generation has been demonstrated at the microjoule level primarily through noncollinear optical parametric amplification (NOPA)[31–35] or optical parametric chirped pulse amplification (OPCPA).[36] These approaches that rely on more involved optical architecture are costly. Alternative methods for generating visible pulses include spectral filtering of continua generated in HCFs,[37] white-light continuum generation via SPM,[38] resonant dispersive wave emission,[39] and multidimensianl solitary states in gas-filled hollow core fiber for visible pulse generation.[40] However, these schemes are often complex due to the involvement of multiple nonlinear effects, including cross-phase modulation (XPM), self-focusing, stimulated Raman scattering, and ionization, and generally require ultrashort input pulses on the order of 30 fs. The interplay of these nonlinearities significantly increases the complexity and sensitivity of the experimental setup.

Here, we present a versatile method to generate ultrashort visible pulses. Our approach employs frequency doubling of the spectrally broadened industrial Yb-laser. The spectrally broadening occurs in a hollow-core fiber system and achieves a spectrum that spans from 800 to 1200 nm. Details of the pump laser system can be found in the supplementary material. From this starting point, we generate the following: (1) tunable sub-50 fs pulses across the 420–600 nm bandwidth, with hundreds microjoule of energy per pulse. Tunability is achieved by tuning phase matching of a single BBO crystal. (2) Tunable sub-20 fs visible pulses with 1–6 μJ energy per pulse across 420–600 nm, and (3) 10 fs visible pulses centered at 530 nm with 3–6 μJ energy per pulse. The shortest pulse duration is achieved using two BBO crystals placed consequently and phase matching different parts of the pump spectrum. In all three cases above, no additional chirped compensation (compression) is required. Making a broadband pump pulse centered at 1030 nm allows us to use simple frequency doubling to generate ultra-short visible pulses. This approach has reduced several nonlinear steps, making it attractive compared to e.g., classical NOPA schemes. The reduced complexity of generation of ultrashort visible pulses will facilitate its integration into a versatile platform for advanced nonlinear experiments.

II. DISCUSSION AND COMPARISON

In this section, we would like to compare our approach to other approaches, starting with the most widespread being OPCPA or NOPA. In recent years, sub 7 fs were readily achieved with these technologies by many groups[41] and even commercialized with multi-TW output powers.[42] These developments, however, were achieved typically at a near-infrared (NIR) wavelength not much shorter than 800 nm. Transferring these concepts toward the visible (VIS) faces challenges of (i) converting the pump wavelength to the blue or UV region and (ii) and increasingly narrower phase matching windows as the nonlinear crystals approach the bandgap. In this regard, the pioneering work of generating 10 fs vis–UV pulses by the Riedle group[31,32] some decades ago has not been topped, to the best of our knowledge. In contrast to NOPAs, the HCF outputs a symmetric beam without spatial chirp, which is preserved in collinear second-harmonic generation (SHG) geometry as is employed in the current work. In terms of system complexity and efficiency, the post-compression of Yb or Ti: Sa lasers, possibly CEP stabilized, clearly possesses advantages over the NOPA route. Extremely broadband OPCPAs are also not widely tunable since the phase matching is engineered at the limit supported by the crystal‘s range, especially when idler absorption becomes relevant.

On the other hand, very broadband frequency doubling had been achieved via achromatic phase matching.[43] In comparison, we believe the simple use of two subsequent BBOs without prism based spectral spreading and recombination denotes a great deal of simplification. A very flexible and powerful conversion employing HCFs is four wave mixing (FWM).[28,44] In this case, yet another HCF needs to be employed together with a multi-color pump–probe setup as the input. Resonant dispersive wave (RDW) emission has also attracted significant interest; however, its efficiency is lower compared to direct SHG processes and its power scalability is limited due to pulse shape distortion at very high peak powers during propagation. Recently, pumping a hollow-core fiber with the frequency-doubled output of a Ti: sapphire laser has demonstrated a promising approach for generating visible pulses with durations as short as 28 fs.[40]

III. THEORY AND NUMERICAL SIMULATIONS

Use of HCF for the generation of the pump for visible light generation allows us to make use of linear spectral phase of the pump. Spectral broadening and the resulting spectral phase evolution in HCFs are predominantly governed by SPM. When the intensity of light propagating through a medium becomes sufficiently high, the refractive index acquires an intensity-dependent

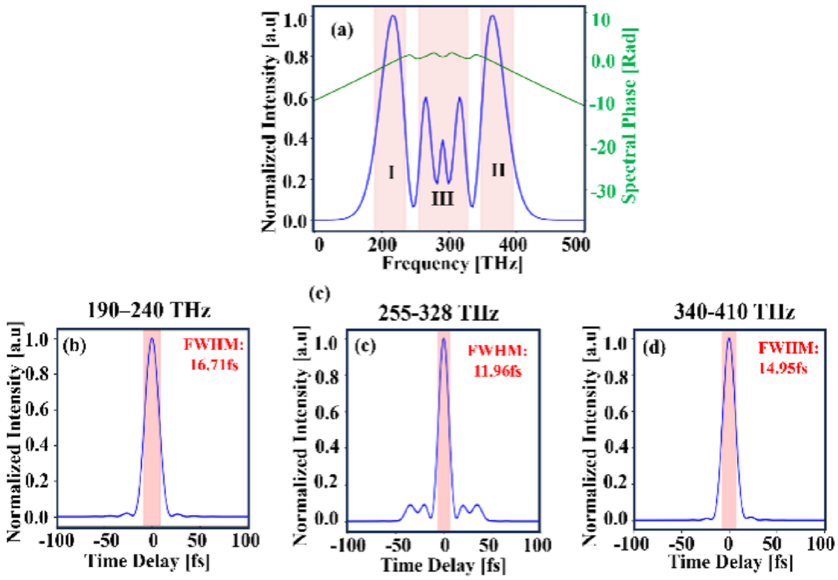

FIG. 1. (a): Spectral broadening and spectral phase evolution induced by self-phase modulation of a 35 fs transform-limited pulse (λ_0 = 1030 nm) after propagation through 1.2 m of argon at 0.2 bar. Three spectral regions were isolated using a fifth-order super-Gaussian filter, and their temporal profiles were retrieved via inverse Fourier transform. Panel (b) represents 190–240 THz, sidelobe; panel (c) represents 255–328 THz, central part of the spectrum; and panel (d) represents 340–410 THz, sidelobe.

term via the Kerr effect, a third-order nonlinear phenomenon. SPM is a direct consequence of this effect: the instantaneous intensity profile of an ultrashort pulse induces a time-dependent refractive index change $\Delta n = n_2 I(t)$, which imparts a nonlinear phase shift $\varphi_{nl}(t) = \frac{\omega_0}{c} n_2 I(t) L$, across the pulse. Here, we demonstrate the spectral broadening of a transform-limited (TL) 36 fs pulse (centered at 1030 nm peak power of 50 GW) by propagating it through a 1.2 m long HCF filled with argon gas at 0.2 bar of absolute pressure. The cross section area is a beam with a diameter of 300 μm. Figure 1(a) represents the spectral broadening and corresponding spectral phase evolution in frequency domains. In the sideband regions of the broadened spectrum (regions I and II), the spectral phase is nearly linear, corresponding to a temporal shift in the time domain. If one were to isolate only this spectral part, close to transform-limited (TL) pulses are to be expected. Upon frequency doubling such a linearly spectrally chirped pulse, the resulting second harmonic inherits a linear spectral phase with twice the slope of the fundamental. Consequently, the second harmonic pulse remains close to TL too, making it suitable for generating ultrashort pulses in the visible range without the need for additional phase compensation (e.g., via chirped mirrors). In the central region (region III), some phase fluctuations are observed. However, after inverse Fourier transforming this region and retrieving its temporal profile, the pulse duration still approaches the transform limit, indicating that phase compensation is unnecessary.

To analyze the temporal behavior, each spectral region was isolated using a fifth-order super-Gaussian filter and subjected to inverse Fourier transformation. As shown in Figs. 1(c) and 1(d), the pulse durations for all three regions closely match the TL calculated from their Gaussian spectral profiles.

This intrinsic ability of SPM to generate broad, linearly spectral phase sidebands not only simplify frequency doubling but also enables efficient difference-frequency generation (DFG) into the mid-infrared with pump at 1030 nm, with the added benefit of inherent carrier-envelope phase stability.[45,46]

IV. EXPERIMENTAL SETUP

A. 8 fs pump generation

Figure 2 provides a depiction of the optical arrangement for generating visible pulses. The output of a Yb: KGW regenerative

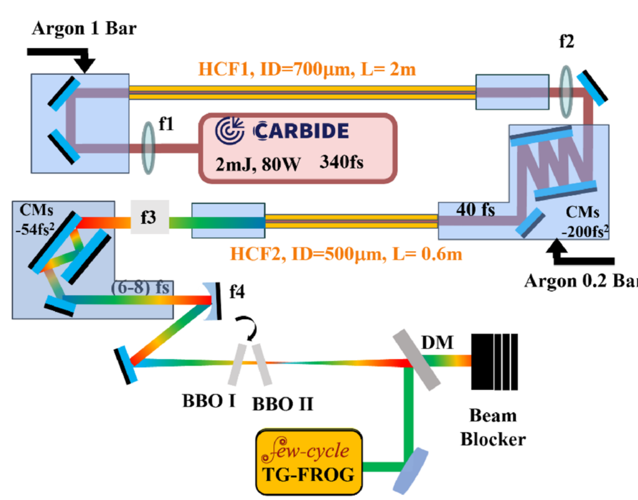

FIG. 2. Schematic of the experimental setup for visible pulse generation. The system consists of a 2 mJ, 340 fs pulse duration Yb: KGW regenerative amplifier (*CARBIDE Light Conversion*), a focusing lens (f1) for coupling into the first hollow-core fiber (HCF1) for spectral broadening, and a second focusing lens (f2) for coupling into the second-stage hollow-core fiber (HCF2). The output of HCF1 is compressed down to 35–40 fs utilizing chirped mirrors (−2000 fs^2, *few-cycle Inc.*), while the output of HCF2 is further compressed down to 6–8 fs using additional chirped mirrors (−58 fs^2; each bounce, *few-cycle Inc.*) and 1.5 mm of fused silica. After collimating the HCF2 output using a 1.5 m focusing mirror (f3), the beam is then focused (f4 = 2 m-focusing mirror) onto two sequential 100 μm thick type-I BBO crystals, cut at 26°, for second harmonic generation. DM: dichroic mirror to remove residual fundamental.

amplifier (*Carbide, Light Conversion*) operating at 80 W average power, 2 mJ, 40 kHz repetition rate, and 340 fs pulse duration was coupled into the first hollow-core fiber (HCF1) (*few-cycle Inc.*) with a core diameter of 700 μm. The laser beam was focused on having ~65% of the fiber's inner diameter (ID) to achieve optimal coupling efficiency in the fundamental mode. HCF1 was filled with argon gas at a relative pressure of 1 bar (2 bars absolute). The output was collimated with a lens and subsequently compressed using chirped mirrors (CMs) with a total dispersion of −2000 fs^2; (−200 fs^2; per bounce at 960–1100 nm, *few-cycle Inc.*). The fiber transmission efficiency was ~90%, after losses of CMs and guiding optics compressed pulse energy is ~1.7 mJ. After compression with CMs, the pulse duration was measured by SHG-FROG (*few-cycle Inc.*) to be 35 fs, which is almost 10-fold compression. By employing a 1.6 m long, 500 μm inner diameter (ID) HCF2 filled with 0.2 bar of krypton gas (relative pressure), the 35 fs pulse underwent spectral broadening while maintaining a coupling efficiency of 70%. Phase compensation was achieved using four bounces on chirped mirrors (~58 fs^2; per bounce, *few-cycle Inc.*) and 1.5 mm of fused silica, resulting in an approximately two-cycle pulse (~6–8 fs) centered at 1030 nm. Further experimental details can be found in Ref. 14. The temporal and spectral characterizations of the HCF2, HCF1 output and Yb laser are shown in Fig. 3.

V. RESULTS

A. Sub 50 fs tunable visible pulse generation

In this experimental scheme, the final set of CMs (−58 fs^2) was removed (Fig. 2) due to the intrinsic linear spectral phase of the SPM process. The pulse was directed through a crystal with 220 μm thickness, type I BBO cut at a 25° angle while being focused by a 2 m concave silver mirror. To prevent crystal damage (50 GW/cm^2), the BBO crystal was positioned 15 cm before the focal point. By adjusting the crystal angle, visible light was generated, tunable in a spectral range of 400–600 nm. After removing the fundamental beam using a combination of two dichroic mirrors, (DMLP650, Thorlabs) and (103922, LAYERTECH, with low GVD), the average power of the generated visible pulses was measured (S142C Thorlabs) to be between 1–5 W at a 40 kHz repetition rate, corresponding to a maximum pulse energy of ~125 μJ at 540 nm (~3 GW). For temporal pulse characterization, Transient Grating FROG (TG-FROG, *few-cycle Inc.*) was employed, revealing pulse durations ranging from 28 to 48 fs. The conversion efficiency of visible pulse generation was measured (Thorlabs S425C-L) to be 6.4%–32%, based on an input power of 15.5 W (before BBO crystal). The spectral tunability of the generated visible pulses and temporal characterization at 480 nm central wavelength using TG-FROG are illustrated in supplementary material, Figs. S.1 and S.2, respectively.

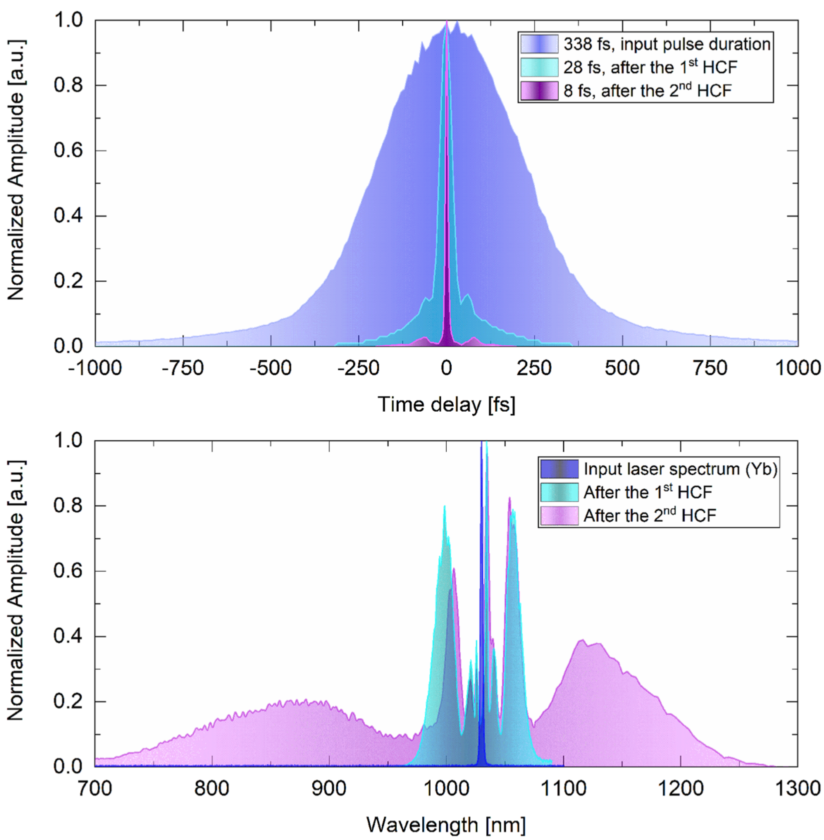

FIG. 3. Temporal characterization: autocorrelation measurements of the input Yb laser and the pulses after the first and second fibers when chirped mirrors (CM) are employed. Spectral broadening: comparison of the spectrum after the second HCF (magenta) with the spectrum after the first HCF stage (cyan) and the input spectrum from the Yb laser (blue).

B. Sub-20 fs tunable visible pulse generation

Because the laser system was shared with another project requiring 10 kHz operation, the results in the following are obtained at the reduced repetition rate. In the case of the thick crystals of Sec. V A, however, we compared operation between 10 and 40 kHz and did not observe any beam modifications due to the increased avg. power. The only observation was a slight phase matching angle adjustment of few degrees. We expect this effect to be lesser in the case of thinner crystals, which exhibit less absorption. In this experimental scheme, the output of the second HCF2 compressed down to 8–10 fs using chirped mirrors. The compressed beam then directed to a type I BBO crystal with a thickness of 100 μm, cut at 26°. The frequency-doubled beam then characterized using the same TG-FROG. The pulse duration of the visible pulse measured to be 15–19 fs, with tunability over the 420–600 nm range. The energy per pulse was measured to be in the range of 1–6 μJ at 10 kHz repetition rage. The spectrum tunability is shown in Fig. 4. The measured TG-FROG trace at 532 nm and reconstructions are shown in Fig. 5. The conversion efficiency of visible pulse generation was measured (Thorlabs S425C-L) to be 1.1%–6.7%, based on an input power of 0.9 W (before BBO crystal). The maximum achieved peak power was measured to be 0.33 GW.

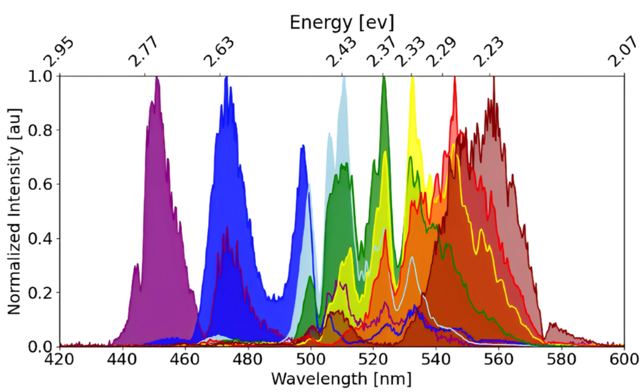

FIG. 4. Represents the normalized spectral tunability within the (420–600) nm range by adjusting the 100 mm BBO crystal angle while it was pumped by 8–10 fs pulses.

Although decreasing the crystal thickness increases the phase matching bandwidth, it compromises the conversion efficiency of the second harmonic generation process. A 50 μm thick, type I BBO crystal was employed, resulting in the generation of 13 fs pulses with a maximum energy of 1.9 μJ per pulse at a 10 kHz repetition rate. This trade-off is due to the reduced interaction length in the crystal, which limits the overall efficiency of the frequency doubling process. In a perfect phase matching condition, the conversion efficiency as function of crystal length is $\varsigma = \frac{\omega d_{eff}^2 L^2 I_\omega}{n_\omega^2 n_{2\omega} \varepsilon_0 c \lambda_\omega^2}$.[47]

C. 10 fs visible pulse generation

We adopted a strategy to overcome the limited phase-matching bandwidth of the BBO crystal (220 μm) while maintaining high conversion efficiency.[48] The same experimental scheme as Sec. V B utilized here. This was achieved by using two type-I BBO crystals cut at 26°, each with a thickness of 100 μm, arranged sequentially in what we refer to as a "***twin***" configuration. One crystal

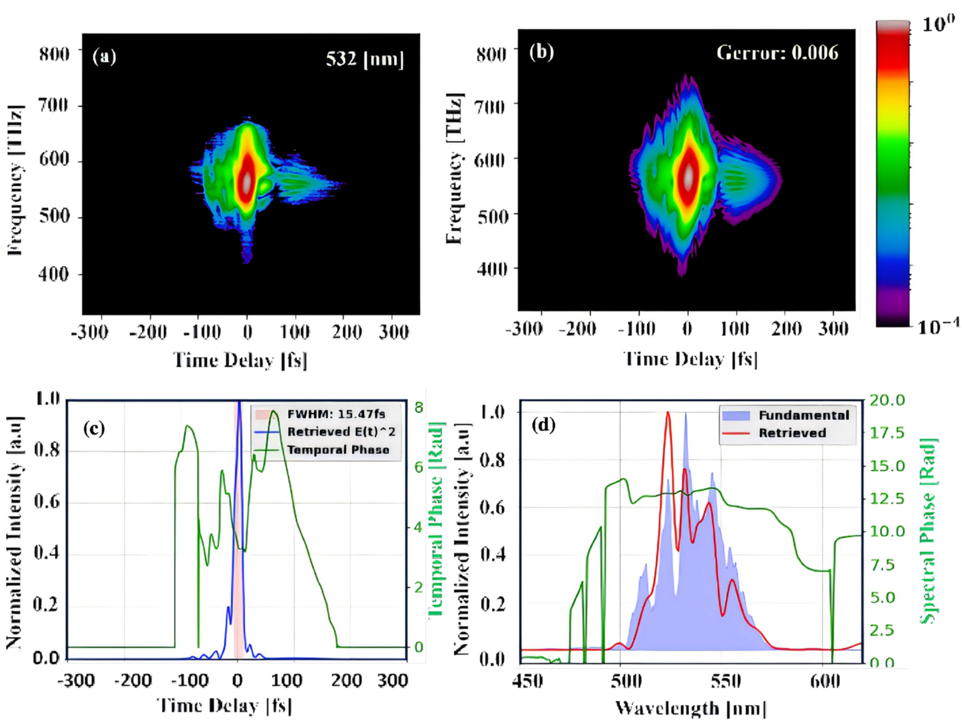

FIG. 5. Panel (a) represents measured TG-FROG trace at 532 nm central wavelength. Panel (b) represents reconstructed trace; panel (c), pulse intensity, which represents a 15.47 fs FWHM; and panel (d) represents a measured and retrieved spectrum.

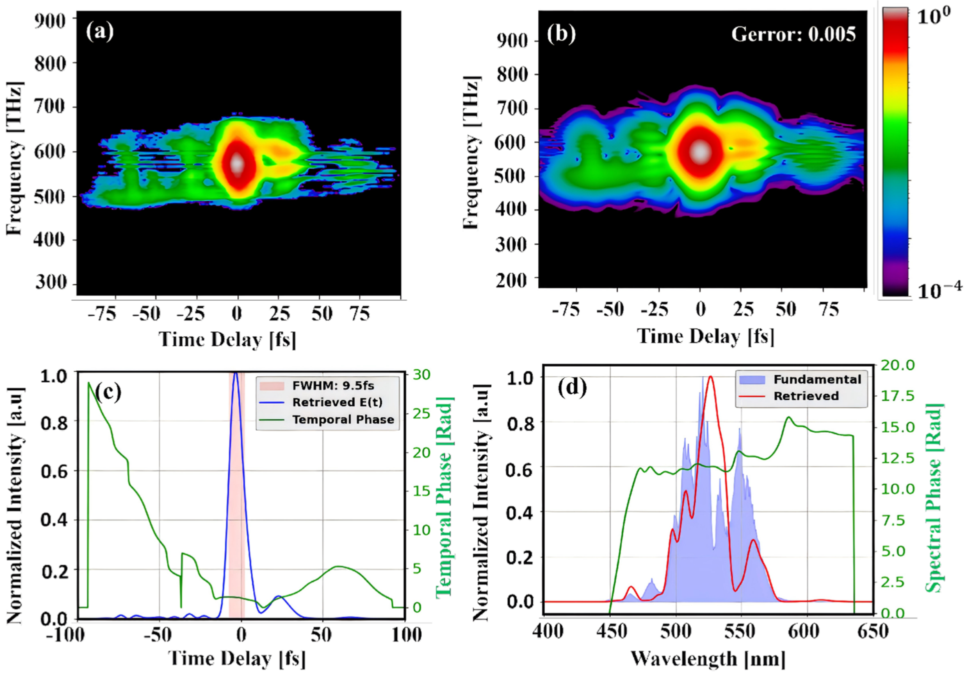

FIG. 6. (a): Measured TG-FROG trace. Panel (b): reconstructed TG-FROG trace with a Gerror of 0.005. Panel (c): retrieved pulse intensity in the time domain, showing pulse duration of 9.5 fs. Panel (d): measured spectrum (blue) and retrieved spectrum (red curve).

was phase-matched to the blue side of the spectrum, while the second crystal was phase-matched to the red side of the spectrum. The two crystals were placed 5 cm apart and 15 cm away from the focus spot of the compressed input beam. This arrangement effectively broadens the phase matching bandwidth while optimizing the conversion efficiency across the entire spectral range. The generated visible (VIS) pulse was spectrally characterized using TG-FROG, and the pulse duration was measured to be ~9.5 fs with 3.1 μJ energy per pulse at 10 kHz repetition rate which corresponds to 0.32 GW. The conversion efficiency of visible pulse generation was measured (Thorlabs S425C-L) to be 3.4%, based on an input power of 0.9 W (before BBO crystal). By applying the principal component generalized projections algorithm (PCGPA),[49,50] the measured TG-FROG trace reconstructed, and its retrieved version are illustrated in Fig. 6.

To evaluate the power stability of the generated visible pulses, long-term power measurements were performed over a 4.5 h period using a silicon-based photodiode power meter (S142CL, Thorlabs). Although power stability was measured for different pulse durations, we present here the results for the 9.5 fs visible pulses, as they are the most susceptible to environmental conditions and optical setup fluctuations. The recorded data showed a relative standard deviation of 0.96% while the mean value of the average power measured 31.07 mW, which demonstrated excellent power stability. The power stability is shown in Fig. 7(a). We chose to present the far-field image of the beam profile, as it more clearly demonstrates the spatial beam quality. Moreover, in many nonlinear optical applications that involve beam focusing, assessing the spatial quality at the focus is more relevant. The spatial beam profile (far-field) was characterized by focusing it with a 1.5 m focal length lens onto a CCD camera. The

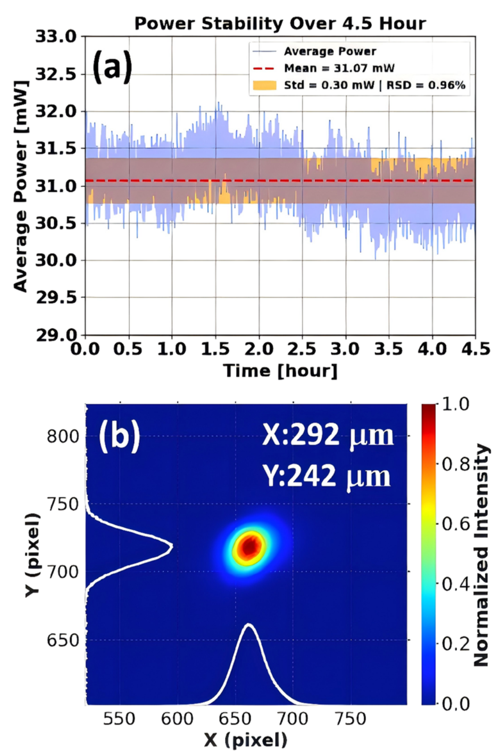

FIG. 7. (a) Thermal stability during continuous running, showing a mean value of 31.07 mW with a relative standard deviation of 0.96%. (b) Far field profile at the focus of a 1.5 m focal length lens. X and Y are $1/e^2$ values.

resulting focal spot is shown in Fig. 7(b). The near-field beam profile also appeared to be clean and approximately Gaussian.

VI. CONCLUSION

In this work, we have demonstrated the generation of high-energy, ultrashort visible pulses with durations ranging from 9.5 to 50 fs and pulse energies spanning from a few to above hundred microjoules. This was achieved by spectrally broadening the output of a narrowband Yb-based laser system and subsequently employing second harmonic generation using single/twin BBO crystal arrangement.

Compared to conventional techniques for visible ultrashort pulse generation, our approach offers significant advantages in terms of simplicity, efficiency, and scalability. The system exhibits excellent long-term power stability, as well as high spatial and temporal beam quality, making it a robust and versatile platform for a wide range of applications in ultrafast science, nonlinear optics, and strong-field physics.

Looking ahead, the availability of high-energy visible pulses from this source paves the way for straightforward extension into the ultraviolet (UV) regime through consequent frequency doubling. This makes the system a promising candidate for future applications requiring intense UV pulses, such as ultrafast spectroscopy, photoemission studies, and attosecond science.

SUPPLEMENTARY MATERIAL

The supplementary material provides the spectral tunability of the generated sub 50 fs visible pulses (Sec. V A) and temporal characterization at 480 nm central wavelength using TG-FROG.

AUTHOR DECLARATIONS

Conflict of Interest

The authors have no conflicts to disclose.

Author Contributions

Pedram Abdolghader: Conceptualization (equal); Data curation (lead); Formal analysis (equal); Methodology (equal); Project administration (equal); Software (supporting); Supervision (lead); Validation (equal); Writing – original draft (lead); Writing – review & editing (equal). **Marco Scaglia**: Data curation (supporting); Formal analysis (equal); Methodology (equal); Project administration (equal); Validation (equal). **Étienne Doiron**: Data curation (supporting); Formal analysis (equal); Methodology (equal); Software (equal); Validation (equal); Writing – review & editing (supporting). **Maksym Ivanov**: Data curation (supporting); Formal analysis (equal); Investigation (equal); Project administration (supporting); Validation (equal); Writing – review & editing (supporting). **Madhu Beniwal**: Data curation (supporting); Formal analysis (supporting); Investigation (supporting); Methodology (supporting); Validation (equal). **Gabriel Tempea**: Investigation (equal); Methodology (equal); Validation (supporting). **Ximeng Zheng**: Data curation (supporting); Formal analysis (equal); Investigation (supporting); Validation (supporting); Writing – review & editing (equal). **Pooya Abdolghader**: Data curation (supporting); Formal analysis (supporting); Software (equal); Validation (supporting); Visualization (equal); Writing – review & editing (supporting). **Giulio Vampa**: Formal analysis (equal); Funding acquisition (equal); Investigation (equal); Methodology (equal); Project administration (equal); Resources (equal). **Bruno E. Schmidt**: Conceptualization (equal); Data curation (supporting); Formal analysis (equal); Funding acquisition (equal); Investigation (equal); Methodology (equal); Project administration (equal); Resources (equal); Supervision (equal); Validation (equal); Writing – original draft (equal); Writing – review & editing (supporting).

DATA AVAILABILITY

The data that support the findings of this study are available from the corresponding author upon reasonable request.

REFERENCES

[1] S. Hädrich, A. Klenke, A. Hoffmann, T. Eidam, T. Gottschall, J. Rothhardt, J. Limpert, and A. Tünnermann, "Nonlinear compression to sub-30-fs, 0.5 mJ pulses at 135 W of average power," Opt. Lett. **38**(19), 3866–3869 (2013).

[2] S. Hädrich, M. Kienel, M. Müller, A. Klenke, J. Rothhardt, R. Klas, T. Gottschall, T. Eidam, A. Drozdy, P. Jójárt, Z. Várallyay, E. Cormier, K. Osvay, A. Tünnermann, and J. Limpert, "Energetic sub-2-cycle laser with 216 W average power," Opt. Lett. **41**(18), 4332–4335 (2016).

[3] J. Weitenberg, A. Vernaleken, J. Schulte, A. Ozawa, T. Sartorius, V. Pervak, H.-D. Hoffmann, T. Udem, P. Russbüldt, and T. W. Hänsch, "Multi-pass-cell-based nonlinear pulse compression to 115 fs at 7.5 μJ pulse energy and 300 W average power," Opt. Express **25**(17), 20502–20510 (2017).

[4] B. Dannecker, J.-P. Negel, A. Loescher, P. Oldorf, S. Reichel, R. Peters, T. Graf, and M. Abdou Ahmed, "Exploiting nonlinear spectral broadening in a 400 W Yb:YAG thin-disk multipass amplifier to achieve 2 mJ pulses with sub-150 fs duration," Opt. Commun. **429**, 180–188 (2018).

[5] H. Fattahi, H. G. Barros, M. Gorjan, T. Nubbemeyer, B. Alsaif, C. Y. Teisset, M. Schultze, S. Prinz, M. Haefner, M. Ueffing, A. Alismail, L. Vámos, A. Schwarz, O. Pronin, J. Brons, X. T. Geng, G. Arisholm, M. Ciappina, V. S. Yakovlev, D.-E. Kim, A. M. Azzeer, N. Karpowicz, D. Sutter, Z. Major, T. Metzger, and F. Krausz, "Third-generation femtosecond technology," Optica **1**(1), 45–63 (2014).

[6] S. Chénais, F. Druon, S. Forget, F. Balembois, and P. Georges, "On thermal effects in solid-state lasers: The case of ytterbium-doped materials," Prog. Quantum Electron. **30**(4), 89–153 (2006).

[7] M. Nisoli, S. De Silvestri, and O. Svelto, "Generation of high energy 10 fs pulses by a new pulse compression technique," Appl. Phys. Lett. **68**(20), 2793–2795 (1996).

[8] S. De Silvestri, M. Nisoli, G. Sansone, S. Stagira, and O. Svelto, *Few-Cycle Pulses by External Compression* (Springer, Berlin, Heidelberg, 2004), pp. 137–178.

[9] B. E. Schmidt, A. Hage, T. Mans, F. Légaré, and H. J. Wörner, "Highly stable, 54 mJ Yb-InnoSlab laser platform at 05 kW average power," Opt. Express **25**(15), 17549–17555 (2017).

[10] Y.-G. Jeong, R. Piccoli, D. Ferachou, V. Cardin, M. Chini, S. Hädrich, J. Limpert, R. Morandotti, F. Légaré, B. E. Schmidt, and L. Razzari, "Direct compression of 170-fs 50-cycle pulses down to 1.5 cycles with 70% transmission," Sci. Rep. **8**(1), 11794 (2018).

[11] J. Schulte, T. Sartorius, J. Weitenberg, A. Vernaleken, and P. Russbueldt, "Nonlinear pulse compression in a multi-pass cell," Opt. Lett. **41**(19), 4511–4514 (2016).

[12] L. Lavenu, M. Natile, F. Guichard, Y. Zaouter, X. Delen, M. Hanna, E. Mottay, and P. Georges, "Nonlinear pulse compression based on a gas-filled multipass cell," Opt. Lett. **43**(10), 2252–2255 (2018).

[13] J. E. Beetar, S. Gholam-Mirzaei, and M. Chini, "Spectral broadening and pulse compression of a 400 μJ, 20 W Yb:KGW laser using a multi-plate medium," Appl. Phys. Lett. **112**(5), 051102 (2018).
[14] M. Ivanov, É. Doiron, M. Scaglia, P. Abdolghader, G. Tempea, F. Légaré, C. A. Trallero-Herrero, G. Vampa, and B. E. Schmidt, "Advancing high-power hollow-core fiber pulse compression," in *IEEE Journal of Selected Topics in Quantum Electronics* (Advances and Applications of Hollow-Core Fibers, 2024), Vol. 30, pp. 1–10.
[15] C.-H. Lu, W.-H. Wu, S.-H. Kuo, J.-Y. Guo, M.-C. Chen, S.-D. Yang, and A. H. Kung, "Greater than 50 times compression of 1030 nm Yb:KGW laser pulses to single-cycle duration," Opt. Express **27**(11), 15638–15648 (2019).
[16] C.-H. Lu, Y.-J. Tsou, H.-Y. Chen, B.-H. Chen, Y.-C. Cheng, S.-D. Yang, M.-C. Chen, C.-C. Hsu, and A. H. Kung, "Generation of intense supercontinuum in condensed media," Optica **1**(6), 400–406 (2014).
[17] M.-S. Tsai, A.-Y. Liang, C.-L. Tsai, P.-W. Lai, M.-W. Lin, and M.-C. Chen, "Nonlinear compression toward high-energy single-cycle pulses by cascaded focus and compression," Sci. Adv. **8**(31), eabo1945 (2022).
[18] A. R. Meadows, K. Yamamoto, I. Graumann, F. Szlafsztein, V. Chvykov, R. Hollinger, C. Aparajit, Z. Shpilman, O. Geiss, P. Abdolghader, B. E. Schmidt, and J. J. Rocca, "Fifteen millijoule, few-cycle pulse compression using a large-bore hollow fiber for relativistic laser–matter interactions," Opt. Lett. **50**(10), 3313–3316 (2025).
[19] T.-C. Truong, D. Khatri, C. Lantigua, C. Kincaid, and M. Chini, "Few-cycle Yb-doped laser sources for attosecond science and strong-field physics," APL Photonics **10**(4), 040902 (2025).
[20] V. Koltalo, S. Westerberg, M. Redon, G. Beaufort, A.-K. Raab, C. Guo, C. L. Arnold, and A.-L. Viotti, "Energy scaling in a compact bulk multi-pass cell enabled by Laguerre–Gaussian single-vortex beams," APL Photonics **10**(4), 040801 (2025).
[21] Y.-G. Jeong, A. Labranche, M. Ivanov, R. Piccoli, L. Zanotto, G. Tempea, P. Abdolghader, R. Morandotti, F. Légaré, L. Razzari, and B. E. Schmidt, "97% throughput hollow-core fibers—For pulse compression of high power Yb lasers," in *2023 48th International Conference on Infrared, Millimeter, and Terahertz Waves (IRMMW-THz)* (IEEE, 2023), pp. 1–2.
[22] G. Fan, P. A. Carpeggiani, Z. Tao, G. Coccia, R. Safaei, E. Kaksis, A. Pugzlys, F. Légaré, B. E. Schmidt, and A. Baltuška, "70 mJ nonlinear compression and scaling route for an Yb amplifier using large-core hollow fibers," Opt. Lett. **46**(4), 896–899 (2021).
[23] T. Nagy, S. Hädrich, P. Simon, A. Blumenstein, N. Walther, R. Klas, J. Buldt, H. Stark, S. Breitkopf, P. Jójárt, I. Seres, Z. Várallyay, T. Eidam, and J. Limpert, "Generation of three-cycle multi-millijoule laser pulses at 318 w average power," Optica **6**(11), 1423–1424 (2019).
[24] M. Reduzzi, M. Pini, L. Mai, F. Cappenberg, L. Colaizzi, F. Vismarra, A. Crego, M. Lucchini, C. Brahms, J. C. Travers, R. Borrego-Varillas, and M. Nisoli, "Direct temporal characterization of sub-3-fs deep UV pulses generated by resonant dispersive wave emission," Opt. Express **31**(16), 26854–26864 (2023).
[25] P. St. J. Russell, P. Hölzer, W. Chang, A. Abdolvand, and J. C. Travers, "Hollow-core photonic crystal fibres for gas-based nonlinear optics," Nat. Photonics **8**(4), 278–286 (2014).
[26] R. Piccoli, J. M. Brown, Y.-G. Jeong, A. Rovere, L. Zanotto, M. B. Gaarde, F. Légaré, A. Couairon, J. C. Travers, R. Morandotti, B. E. Schmidt, and L. Razzari, "Intense few-cycle visible pulses directly generated via nonlinear fibre mode mixing," Nat. Photonics **15**(12), 884–889 (2021).
[27] H. Zhang, L.-S. Sun, J. Hirschman, M. S. Shariatdoust, F. Belli, and S. Carbajo, "Optimizing spectral phase transfer in four-wave mixing with gas-filled capillaries," Opt. Express **32**(25), 44397–44412 (2024).
[28] C. G. Durfee, S. Backus, H. C. Kapteyn, and M. M. Murnane, "Intense 8-fs pulse generation in the deep ultraviolet," Opt. Lett. **24**(10), 697–699 (1999).
[29] A. Lekosiotis, F. Belli, C. Brahms, T. Grigorova, H. Sakr, I. A. Davidson, F. Poletti, and J. C. Travers, "Progress in ultrafast optics using hollow-core fibres," in *Optica Advanced Photonics Congress 2022* (Optica Publishing Group, 2022), p. SoTu4I.2.
[30] R. L. Fork, C. H. Brito Cruz, P. C. Becker, and C. V. Shank, "Compression of optical pulses to six femtoseconds by using cubic phase compensation," Opt. Lett. **12**(7), 483–485 (1987).
[31] E. Riedle, M. Beutter, S. Lochbrunner, J. Piel, S. Schenkl, S. Spörlein, and W. Zinth, "Generation of 10 to 50 fs pulses tunable through all of the visible and the NIR," Appl. Phys. B **71**(3), 457–465 (2000).
[32] T. Wilhelm, J. Piel, and E. Riedle, "Sub-20-fs pulses tunable across the visible from a blue-pumped single-pass noncollinear parametric converter," Opt. Lett. **22**(19), 1494–1496 (1997).
[33] G. Cerullo, M. Nisoli, S. Stagira, and S. De Silvestri, "Sub-8-fs pulses from an ultrabroadband optical parametric amplifier in the visible," Opt. Lett. **23**(16), 1283–1285 (1998).
[34] A. Baltuška, T. Fuji, and T. Kobayashi, "Visible pulse compression to 4 fs by optical parametric amplification and programmable dispersion control," Opt. Lett. **27**(5), 306–308 (2002).
[35] J. H. Odhner and R. J. Levis, "High-energy noncollinear optical parametric amplifier producing 4 fs pulses in the visible seeded by a gas-phase filament," Opt. Lett. **40**(16), 3814–3817 (2015).
[36] A. Harth, M. Schultze, T. Lang, T. Binhammer, S. Rausch, and U. Morgner, "Two-color pumped OPCPA system emitting spectra spanning 15 octaves from VIS to NIR," Opt. Express **20**(3), 3076–3081 (2012).
[37] A. Wirth, M. Th. Hassan, I. Grguraš, J. Gagnon, A. Moulet, T. T. Luu, S. Pabst, R. Santra, Z. A. Alahmed, A. M. Azzeer, V. S. Yakovlev, V. Pervak, F. Krausz, and E. Goulielmakis, "Synthesized light transients," Science **334**(6053), 195–200 (2011).
[38] E. Matsubara, K. Yamane, T. Sekikawa, and M. Yamashita, "Generation of 26 fs optical pulses using induced-phase modulation in a gas-filled hollow fiber," J. Opt. Soc. Am. B **24**(4), 985–989 (2007).
[39] J. C. Travers, T. F. Grigorova, C. Brahms, and F. Belli, "High-energy pulse self-compression and ultraviolet generation through soliton dynamics in hollow capillary fibres," Nat. Photonics **13**(8), 547–554 (2019).
[40] M. Kumar, M. Arshadipirlar, R. Safaei, H. Ibrahim, and F. Légaré, "Generating ultrashort visible light pulses based on multidimensional solitary states in gas-filled hollow core fiber," APL Photonics **8**(5), 056104 (2023).
[41] F. J. Furch, T. Witting, A. Giree, C. Luan, F. Schell, G. Arisholm, C. P. Schulz, and M. J. J. Vrakking, "CEP-stable few-cycle pulses with more than 190 μJ of energy at 100 kHz from a noncollinear optical parametric amplifier," Opt. Lett. **42**(13), 2495–2498 (2017).
[42] S. Toth, T. Stanislauskas, I. Balciunas, R. Budriunas, J. Adamonis, R. Danilevicius, K. Viskontas, D. Lengvinas, G. Veitas, D. Gadonas, A. Varanavičius, J. Csontos, T. Somoskoi, L. Toth, A. Borzsonyi, and K. Osvay, "SYLOS lasers—The Frontier of few-cycle, multi-TW, kHz lasers for ultrafast applications at extreme light infrastructure attosecond light pulse source," J. Phys.: Photonics **2**(4), 045003 (2020).
[43] P. Baum, S. Lochbrunner, and E. Riedle, "Tunable sub-10-fs ultraviolet pulses generated by achromatic frequency doubling," Opt. Lett. **29**(14), 1686–1688 (2004).
[44] P. Zuo, T. Fuji, and T. Suzuki, "Spectral phase transfer to ultrashort UV pulses through four-wave mixing," Opt. Express **18**(15), 16183–16192 (2010).
[45] E. Doiron, M. Ivanov, M. Scaglia, P. Ghaderi, G. Vampa, G. Tempea, F. Legare, and B. E. Schmidt, "HYPUS: Hyperspectral ultrafast source," Proc. SPIE **PC13347**, PC133470I (2025).
[46] L. Xu, Ch. Spielmann, A. Poppe, T. Brabec, F. Krausz, and T. W. Hänsch, "Route to phase control of ultrashort light pulses," Opt. Lett. **21**(24), 2008–2010 (1996).
[47] R. W. Boyd, "Chapter 2—Wave-equation description of nonlinear optical interactions," in *Nonlinear Optics*, 4th ed., edited by R. W. Boyd (Academic Press, 2020), pp. 65–135.
[48] Y. Li, B. Shao, Y. Peng, J. Qian, W. Li, X. Wang, X. Liu, X. Lu, Y. Xu, Y. Leng, and R. Li, "Ultra-broadband pulse generation via hollow-core fiber compression and frequency doubling for ultra-intense lasers," High Power Laser Sci. Eng. **11**(1), 010000e5 (2023).
[49] D. J. Kane, G. Rodriguez, A. J. Taylor, and T. S. Clement, "Simultaneous measurement of two ultrashort laser pulses from a single spectrogram in a single shot," J. Opt. Soc. Am. B **14**(4), 935–943 (1997).
[50] D. J. Kane, "Recent progress toward real-time measurement of ultrashort laser pulses," IEEE J. Quantum Electron. **35**(4), 421–431 (1999).